Electronic Supplementary Material (ESI) for Green Chemistry.

Synergistic Catalysis of Tandem Li/S-1 and Sn-Beta Catalysts for the Conversion of Glucose to Fructose and Lactic acid at 90 °C in Water

Yanfei Zhang [a,b,&], Wanting Li [a,b,&], Wenqian Li [a,b], Yanfeng Zhu [a], Longfei Chen [a,b], Gai Miao[a], Hu Luo[a,*], Xinqing Chen [a,b,*], Lingzhao Kong [a,b,c,*]

[a] CAS Key Laboratory of Low-Carbon Conversion Science and Engineering, Shanghai Advanced Research Institute, Chinese Academy of Sciences, Shanghai 201210 (P.R. China)

[b] University of Chinese Academy of Sciences, Beijing 100049 (P.R. China)

[c] School of Environmental Science and Engineering, Suzhou University of Science and Technology, Suzhou, Jiangsu, 215009, P.R. China.

[&] These two authors contribute equally

*Corresponding authors: (chenxq@sari.ac.cn, luoh@sari.ac.cn, konglz@sari.ac.cn)

General Information

All chemicals were used as received from the commercial suppliers:, mannose (≥99%), fructose (≥99 %), LiCl (AR, ≥99.0 %), glucose (AR, 99.0 %),lactic acid(AR，≥99%), formic acid (AR, ≥99 %),. All reactions were performed in a 100.0 mL Parr pressure reactor. Centrifugation of the reaction mixture was performed on Thermo LYNX6000 (3000 rpm, 10 min).

Carbon-13 Nuclear Magnetic Resonance Spectrometry (^{13}C NMR): Agilent 500 MHz (125MHz), The product was dissolved in D_2O and scanned 1024 times.

X-Ray powder diffraction (XRD) patterns of the catalysts were performed on Rigaku Ultima IVX-Ray diffractometer using Cu Kα radiation in the 2θ range from 5 ° to 80 ° at a scan rate of 2°/min.

Scanning electron microscope (SEM) analysis: The Supra 55 Sapphire field emission scanning electron microscope of Carl Zeiss (shanghai) Co was used to analyze the morphology of the catalyst. The test voltage was 15 KV, catalyst powder needed to be taken for gold spraying before the test.

Pyridine adsorption Fourier-transform infrared (Py-IR): The catalyst was detected by the FT-IR Nicolet 670. Weigh out 0.05 g of catalyst, press it into a translucent sheet in a tablet press, and place it in the sample tank (the material of the sample tank and the window is quartz). The sample tank was evacuated and treated at 200 °C for 2 h, after which the temperature was lowered to room temperature and the sample background spectrum was measured. Firstly, the pyridine gas is introduced into the sample tank to absorb the saturation of the sample. Raise the sample temperature to 200 °C and hold it for 1 h to measure the spectrum at 200 °C. After that, the temperature was increased to 350 °C for 1 h, and infrared spectra of pyridine adsorption at 200 °C and 350 °C were obtained.

Analysis of specific surface area of nitrogen adsorption (BET): Micromeritics, TriStar Ⅱ3020, The sample to be tested is first degassed at 300 °C for more than 3 h, and then tested with N_2 as the medium at -196 °C.

Inductively coupled plasma-atomic emission spectrometry (ICP): Perkin Elmer Optima 8000, digest and filter a certain amount of catalyst to measure the content of Li.

UV Vis absorption spectrum: Agilent Spectrophotometer technologies Cary 5000 UV vis-NIR, measuring wavelength range: 200-500 nm.

Total Organic Carbon (TOC): Shimadzu TOC-LCSH/CPH, Liquid products need to be diluted, range : 4 μg/L~30000 mg/L. According to the TOC results, the carbon balance was >99.9 % in 90 °C.

The data were recorded on the HPLC (Shimadzu LC-20A, Aminex HPX-87H Ion Exclusion Column: 300 mm × 7.8 mm. RID-10A). Analysis condition: column temperature 50 °C, injection volume 10 μL, the mobile phase 12.5 mmol/L H_2SO_4, 0.60 ml/min. After reaction, the solids were separated by filtration and the composition of the liquid phase was analyzed by HPLC. Besides the main product fructose and lactic acid, a variety of other compounds were detected in more than 120 °C, which were comprehensively analyzed. By drawing a standard working curve with the standard product of the specific component to be tested, and then measuring the content of the component in the sample under the exact same chromatographic conditions, the concentration can be found from the working curve. Conversion and yield values were calculated based on the equations shown in the quantification part.

Recycling Test

After a typical catalytic run (200 mg catalysts, 20 ml water, 90 °C, 1 h, 0.1 MPa N_2), the catalyst was separated from the reaction solution by centrifugation and subsequent decantation. The solid was additionally washed with water and dried overnight at room temperature under vacuum prior to the next run.

Preparation of Li/S-1 catalyst

S-1 zeolite preparing: Accurately weigh 23.5 g TEOS, 36.7 g TPAOH (25 %) and 33.9 g H_2O mix well. Stir while reacting at room temperature for 6 h. After the reaction, transfer it to the crystallizing kettle, and put it into the oven at 170 °C for 3 days. After taking it out, it was washed and centrifuged, dried and baked at 550 °C for 3 h.
Li/S-1 catalyst preparing: Take 2.0 g S-1 zeolite and 0.12 g LiCl into bowl and carefully grand for 30 min, then put the mixture into muffle furnace and baked at 550 °C for 3 h.

Preparation of Sn-Beta catalyst

Accurately weigh 30.6 g TEOS and 33.1 g TEAOH (35 %) and mix well. Stir while reacting at room temperature for 2 h. After the reaction, add 0.257 g $SnCl_4$ and continue stirring for 1 h. During the stirring process, add 0.3 wt% of dealuminated molecular sieve seed crystals, and then evaporate the ethanol and part of the water to make the material reach the following ratio: 1 SiO_2: 0.005 $SnCl_4$: 0.55 TEAOH: 0.55 HF: 7.5 H_2O. Add 3.97 g HF, the material liquid changes from sol state to solid gel, transfer it to the crystallizing kettle, and put it into the oven at 140 °C for 7 days. After taking it out, it was washed by suction filtration, dried and baked at 550 °C for 6 h.

Quantification

The yield of products was calculated based on the number of carbons in the product as follows: where represents the number of carbons and C_i is the molar concentration of the compound i, $C_{glucose}$ indicates molar concentration of glucose before the reaction.

$$\text{Yield } /\% = (C_i / C_{glucose}) \times 100\ \%$$

Conversion was based on the molar carbon concentration of the compounds according to the equations below, where $C_{glucose}$ indicates the molar carbon concentration of glucose before the reaction and $C_{glucose}$' indicates the molar carbon concentration of glucose after the reaction.

$$\text{Conversion } /\% = (C_{glucose} - C_{glucose}') / C_{glucose} \times 100\ \%$$

Selectivity was based on the molar carbon concentration of the compounds according to the equations below, where $C_{glucose}$ indicates the molar carbon concentration of glucose before the reaction and $C_{glucose}$' indicates the molar carbon concentration of glucose after the reaction. C_i indicates molar carbon concentration of compound i.

$$\text{Selectivity } /\% = C_i / (C_{glucose} - C_{glucose}') \times 100\ \%$$

Conversion of glucose

In a typical experiment, the catalyst (200 mg unless otherwise stated) and 200 mg glucose were placed in an intermittent high-pressure reactor (100 mL), and deionized water (20 mL) were added. Initially, the reactor necessitates the use of N_2 for purging air, with the gas exchange procedure repeated five times to ensure complete removal of atmospheric constituents. Subsequently, the reactor should be tightly sealed, facilitating thorough catalyst interaction with the reactants via mechanical stirring once the desired reaction temperature is attained. Upon completion of the reaction, the heating sleeve is removed, and the reactor is rapidly cooled using ice water.

Computational Details:

All geometric optimizations have been carried out by density functional theory using the B3LYP hybrid functional [1] with Grimme's dispersion correction of D3 version (Becke-Johnson damping) [2]. The standard 6-31G(d,p) basis set[3-5] for H, C, O and Si atoms was used. For the Sn atom, the SDD basis set and its corresponding effective core potential [6] was used. Frequency calculations at the same level of theory have also been performed to identify all stationary points as minima (zero imaginary frequencies) and transition states (one imaginary frequencies). The intrinsic reaction coordinate (IRC) scheme [7-8] was applied for the calculations of the reaction coordinates to confirm whether or not the transition states were directly connected to the reactants and products. The single-point energy (SP) calculations were performed on the optimized geometries at def2-TZVP basis set [9-10]. Approximate solvent effects were taken into consideration based on the continuum solvation model in optimization [11] and SP [12] calculations. All the above calculations were carried out by Gaussian 16 programs [13].

Table S1: The conversion results of different reactants over Sn-Beta and Li/S-1 catalyst.

Stocks	Stocks	Lactic acid %	Fructose %
cellulose	Sn-Beta	0	0
xylose	Sn-Beta	2.1	0
glyceraldehyde	Sn-Beta	91.3	0
mannose	Sn-Beta	0	11.7
1,3-dihydroxyacetone	Sn-Beta	87.8	0
cellulose	Li/S-1	0	0
xylose	Li/S-1	0	0
glyceraldehyde	Li/S-1	3.1	0
mannose	Li/S-1	0	0
1,3-dihydroxyacetone	Li/S-1	2.3	0

Reaction condition: 1 h, 0.1 MPa N_2, 200 mg glucose, 200 mg catalyst, 20 mL H_2O and 90 °C. The Li and Sn loading is 1 wt% in all experiments.

Table S2. The conversion results of different solvent over Sn-Beta and Li/S-1 catalyst.

	Solvent	Conversion %	Yield %	Selectivity %
1	H_2O	83	33	40
2	Methanol	-	-	-
3	Ethanol	-	-	-
4	Glycerol	-	-	-
5	γ-Valerolactone	-	-	-

Reaction condition: 1 h, 0.1 MPa N_2, 200 mg glucose, 200 mg catalyst, 20 mL solvent and 90 °C. The Li and Sn loading is 1 wt% in all experiments.

Table S3. ICP of Sn-Beta and Li/S-1 catalyst.

Catalysts	M % (Theoretical loading)	M % (After washing)	M % (After reaction)
Li/S-1	1.0wt%	0.78wt%	0.77wt%
Sn-Beta	1.0wt%	0.81wt%	0.80wt%

Table S4. BET of Li/S-1 and Sn-Beta catalyst

Catalysts	BET surface/m^2•g	Pore width/nm
S-1	359.1501	3.03991
0.5 Li/S-1	301.8382	3.32120
1 Li/S-1	289.9329	3.28832
2 Li/S-1	292.6884	3.10826
Sn-Beta	460.9132	4.41353

Table S5. Py-IR analysis of Sn-Beta catalyst.

Sample	Brønsted site density (mmol g^{-1})		Lewis site density (mmol g^{-1})	
	200 °C	350 °C	200 °C	350 °C
Sn-Beta-W	0.018	0.016	0.231	0.073

Total*: Total acid content in catalyst, The Li loading is 1 wt% in all experiments.

B/L*: The mass ratios of Brønsted acid: Lewis-acid.

Table S6. EXAFS fitting parameters at the Sn K-edge for various samples.

Sample	Shell	*CN*[a]	*R*(Å)[b]	σ^2(Å^2)[c]	ΔE_0(eV)[d]	*R* factor
Sn foil	Sn-Sn	8*	3.01	0.0120	2.21	0.0036
SnO_2	Sn-O	7.7	2.04	0.0028	5.01	0.0159
	Sn-Sn1	4.0	3.19	0.0065	2.60	
	Sn-Sn2	7.1	3.75	0.0030	9.92	
Sn-Beta	Sn-O	6.0	1.99	0.0043	3.55	0.0058

[a]CN, coordination number; [b]R, distance between absorber and backscatter atoms; [c]σ^2, Debye-Waller factor to account for both thermal and structural disorders; [d]ΔE_0, inner potential correction; R factor indicates the goodness of the fit. S_0^2 was fixed to 0.81. A reasonable range of EXAFS fitting parameters: $0.600 < S_0^2 < 1.000$; CN > 0; $\sigma^2 > 0$ Å^2; |ΔE0| < 10 eV; R factor < 0.02。

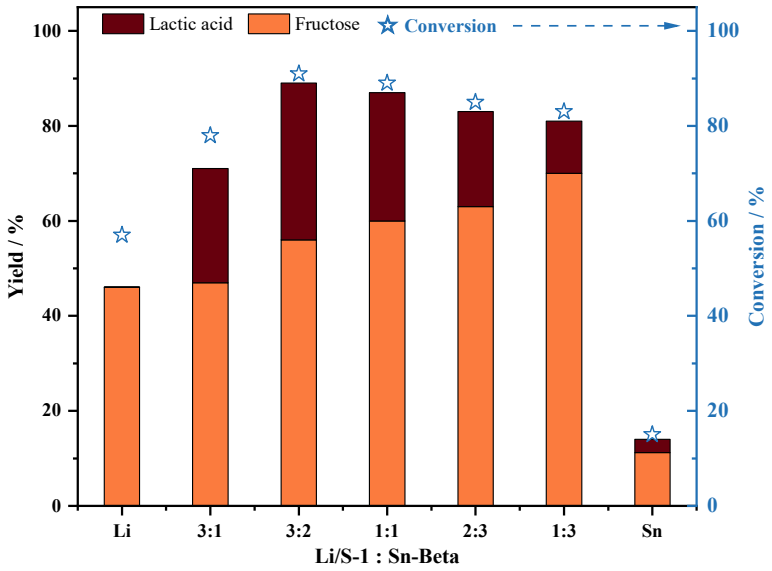

Figure S1. The results of different ratio between Li/S-1 and Sn-Beta catalyst. Reaction conditions: 90 °C, 1h, 0.2g feedstocks, 0.2g catalyst with the different ratio of Li/S-1 to Sn-Beta, 1% Li loaded S-1 zeolite and 1% Sn loaded Beta zeolite, 0.1 MPa N_2.

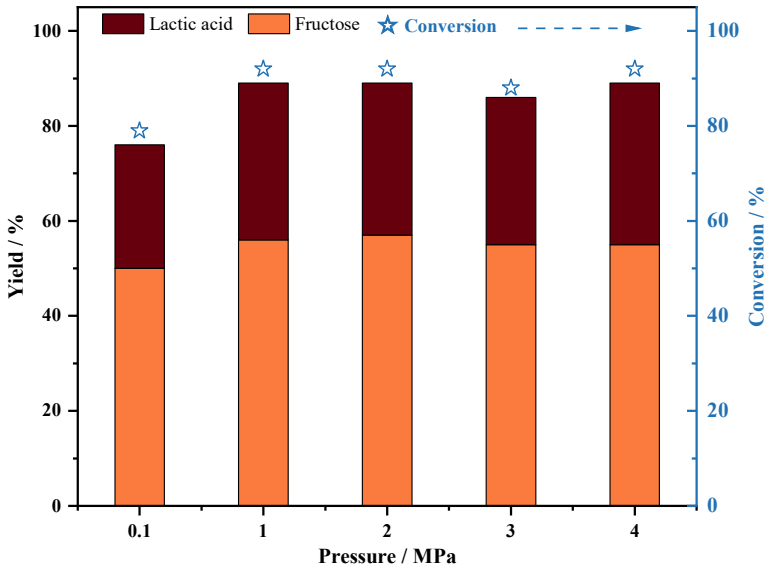

Figure S2. The results of different pressure over Li/S-1 & Sn-Beta catalyst. Reaction conditions: 90 °C, 1h, 0.2g feedstocks, 0.2g catalyst with the 3:2 ratio of Li/S-1 to Sn-Beta, 1% Li loaded S-1 zeolite and 1% Sn loaded Beta zeolite.

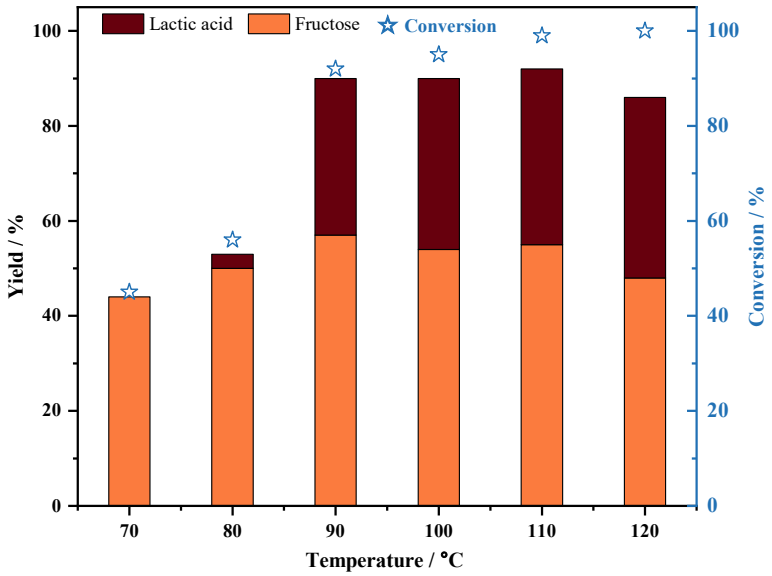

Figure S3. The results of different temperature over Li/S-1 & Sn-Beta catalyst. Reaction conditions: 1h, 0.2g stocks, 0.2g catalyst with the 3:2 ratio of Li/S-1 to Sn-Beta, 1% Li loaded S-1 zeolite and 1% Sn loaded Beta zeolite, 0.1 MPa N_2.

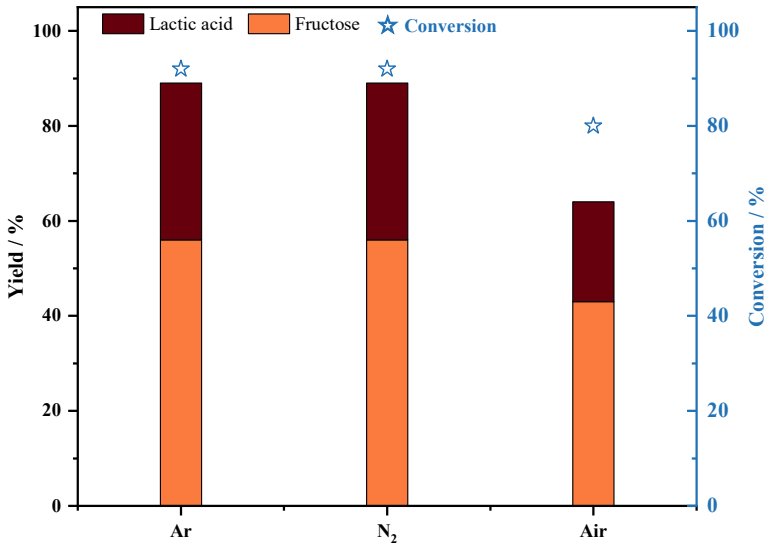

Figure S4. The results of different gas over Li/S-1 & Sn-Beta catalyst. Reaction conditions: 90 °C, 1h, 0.2g stocks, 0.2g catalyst with the 3:2 ratio of Li/S-1 to Sn-Beta, 1% Li loaded S-1 zeolite and 1% Sn loaded Beta zeolite, (Air, Ar)0.1 MPa and 0.1 MPa N_2.

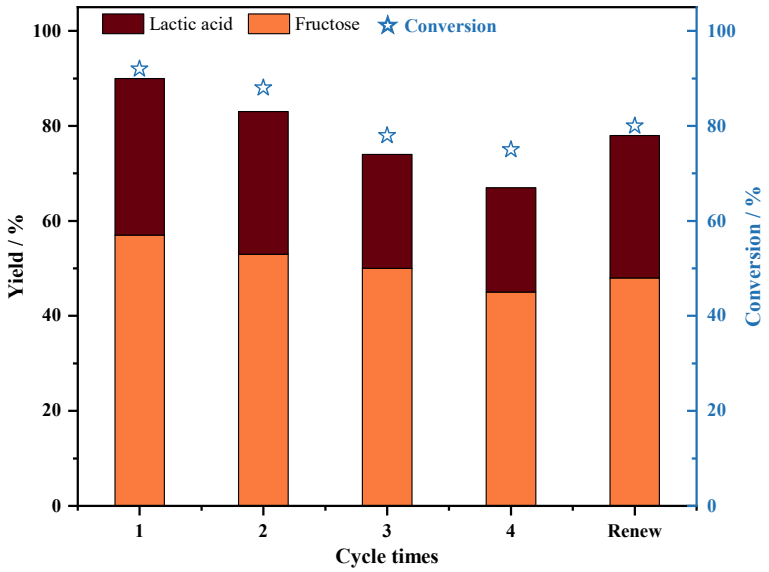

Figure S5. The results of glucose conversion over Li/S-1 & Sn-Beta catalyst in 4 cycles. Reaction conditions: Reaction conditions: 90 °C, 1h, 0.2g stocks, 0.2g catalyst with the 3:2 ratio of Li/S-1 to Sn-Beta, 1% Li loaded S-1 zeolite and 1% Sn loaded Beta zeolite, 0.1 MPa N_2.

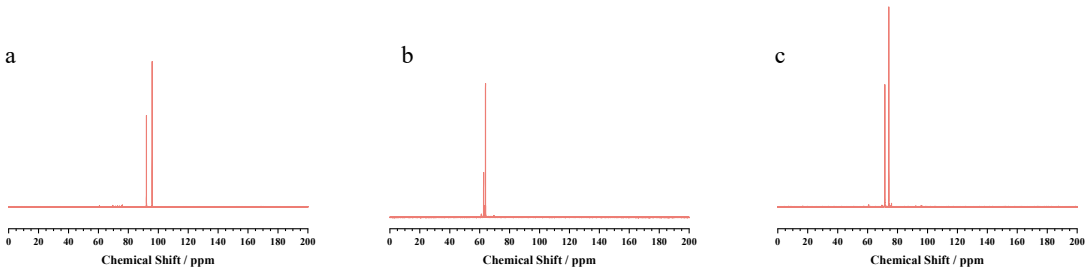

Figure S6. The ^{13}C NMR analysis of C1-glucose(a) C1-Fructose (b) and C2-glucose (c)

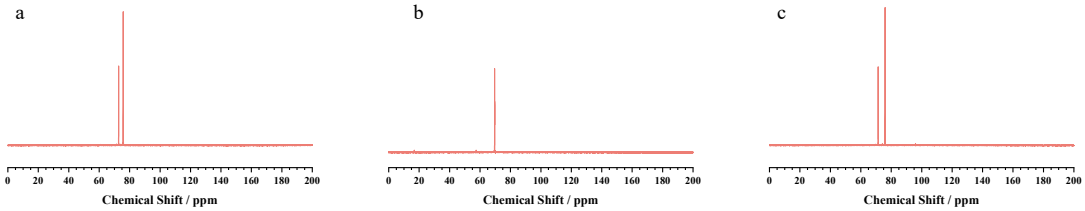

Figure S7. The ^{13}C NMR analysis of C3-Fructose (a) C4-Fructose (b) and C5-Fructose (c)

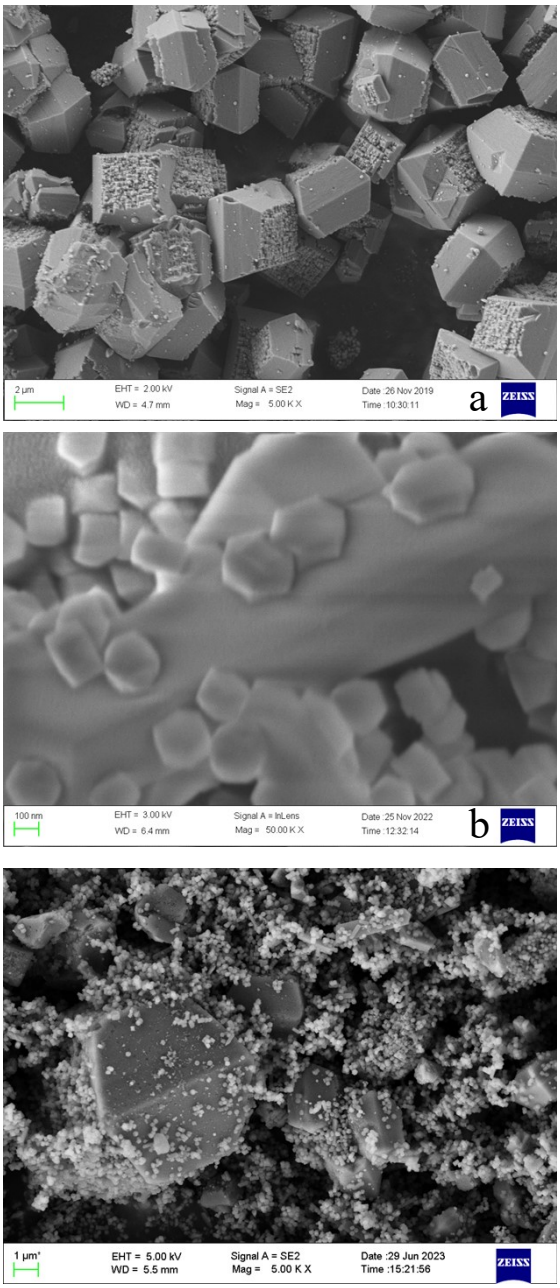

Figure S8. SEM image of Sn-Beta catalyst (a), Li/S-1 catalyst (b) and PX catalysts(c)

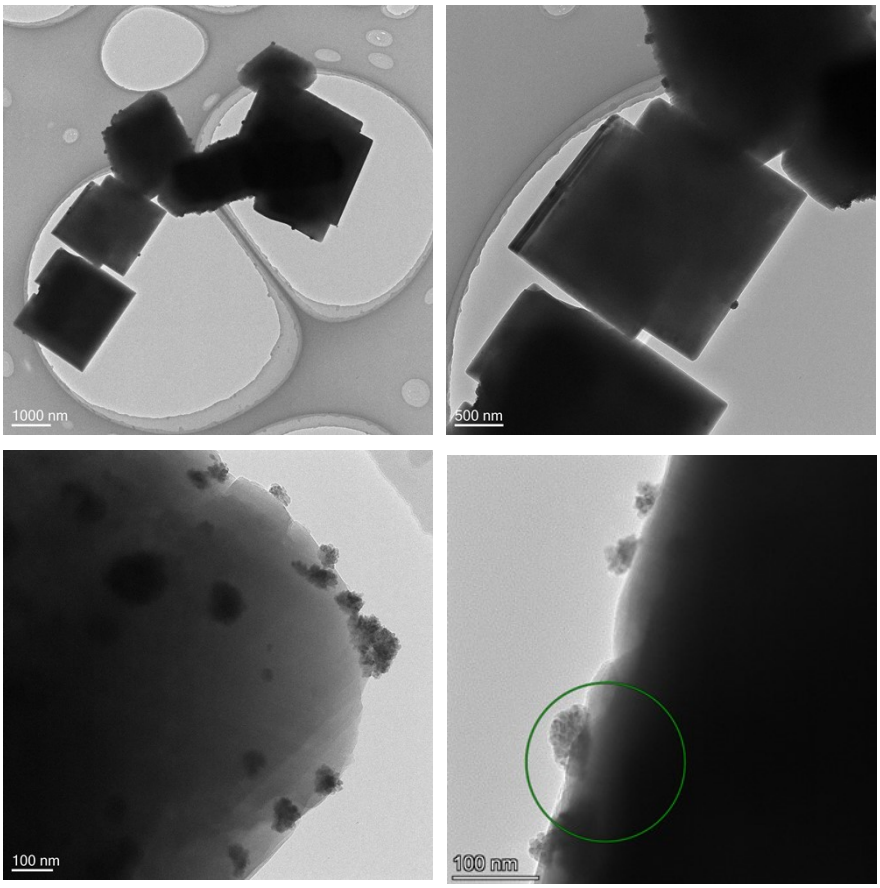

Figure S9. The TEM images of Sn-Beta catalyst.

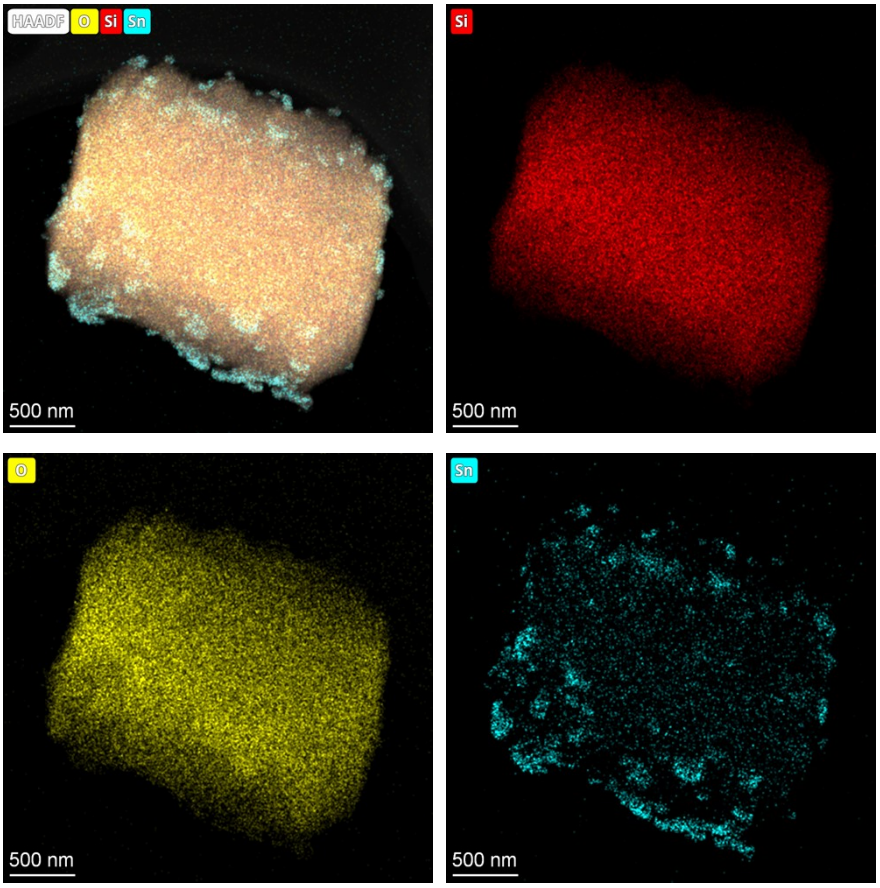

Figure S10. The element mapping of Sn-Beta catalyst.

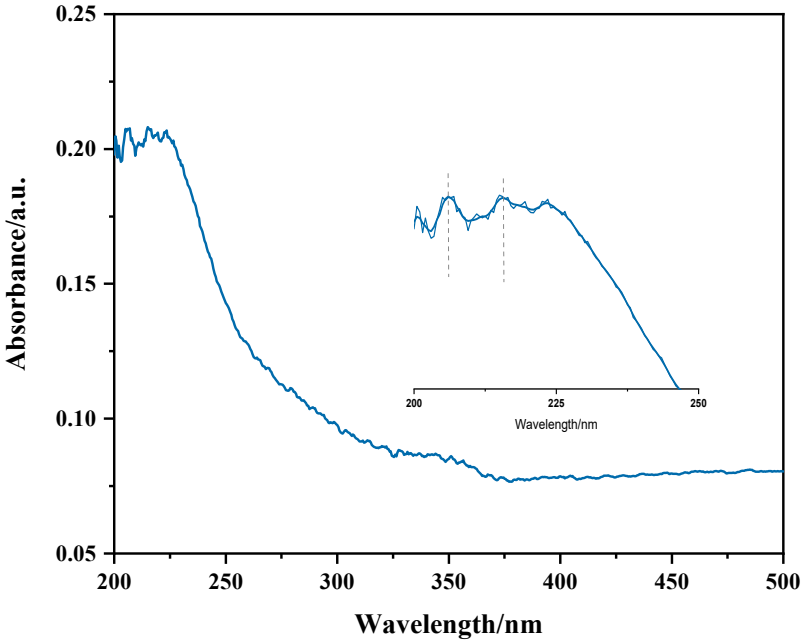

Figure S11. UV-Vis analysis of Sn-Beta catalyst.

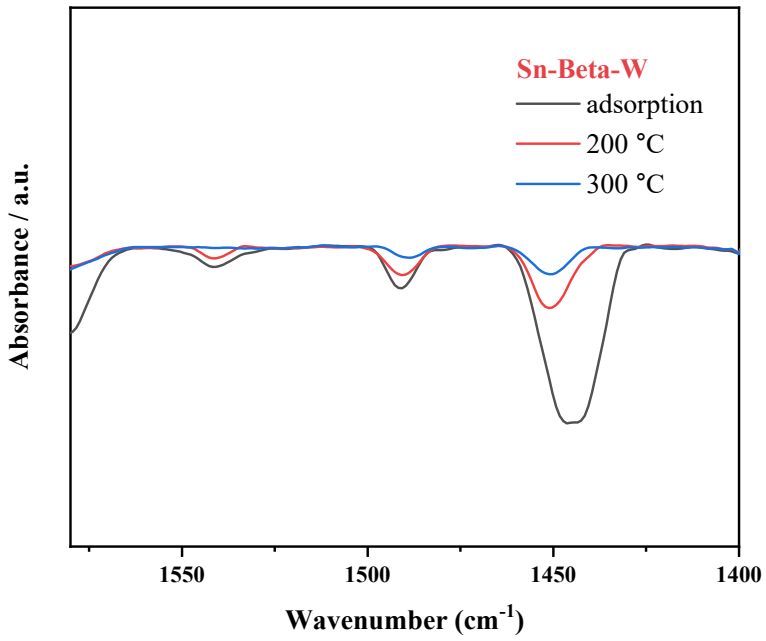

Figure S12. Py-IR analysis of Sn-Beta catalyst

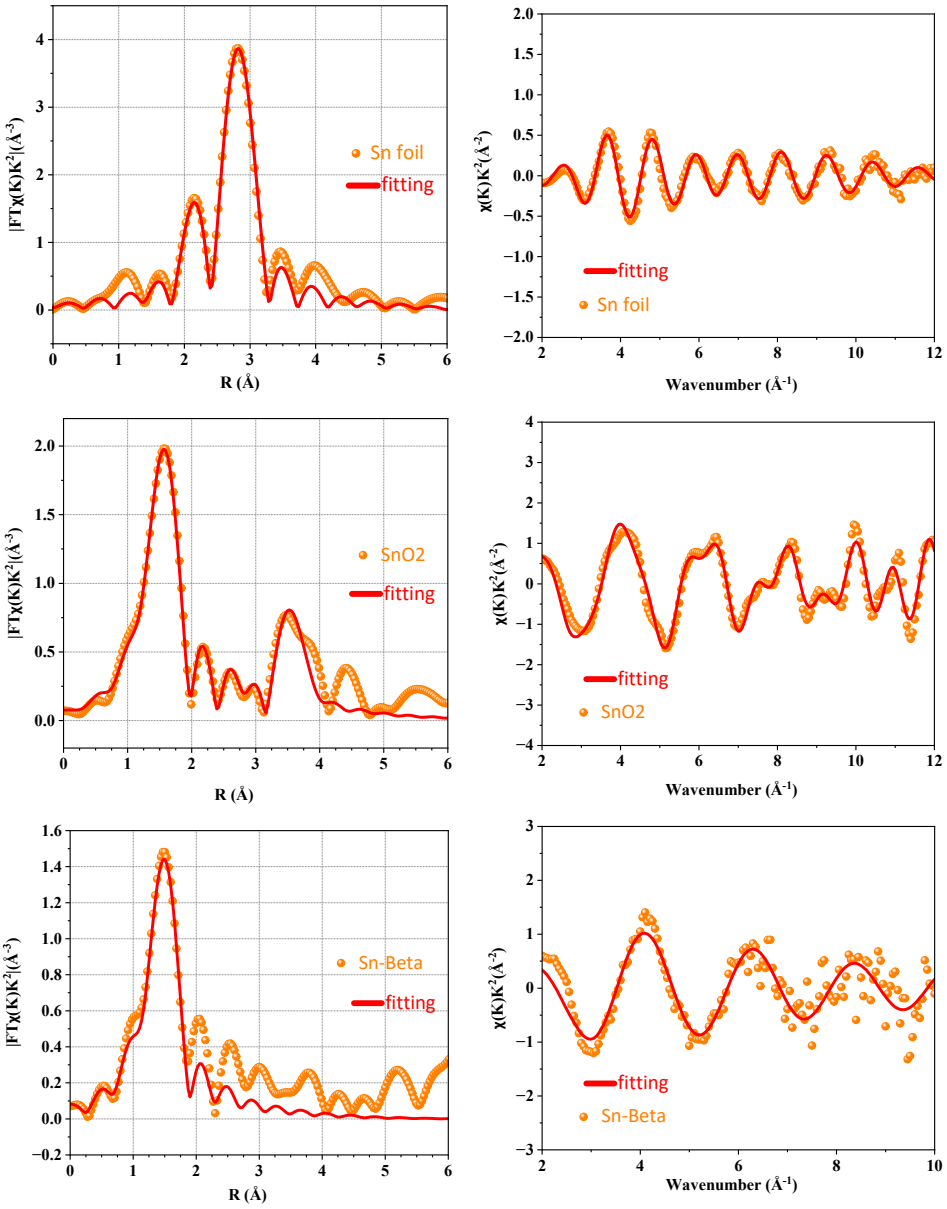

Figure S13. EXAFS R-space and K-space fitting curve of Sn-Beta catalyst

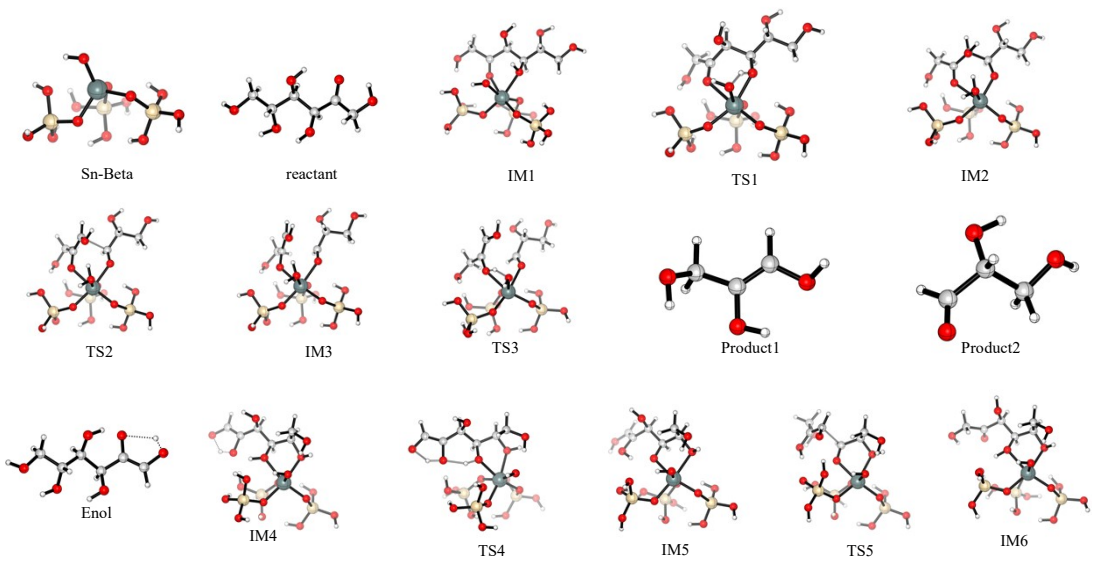

Figure S14. Adsorption Models of Reactants on Sn-Beta catalyst

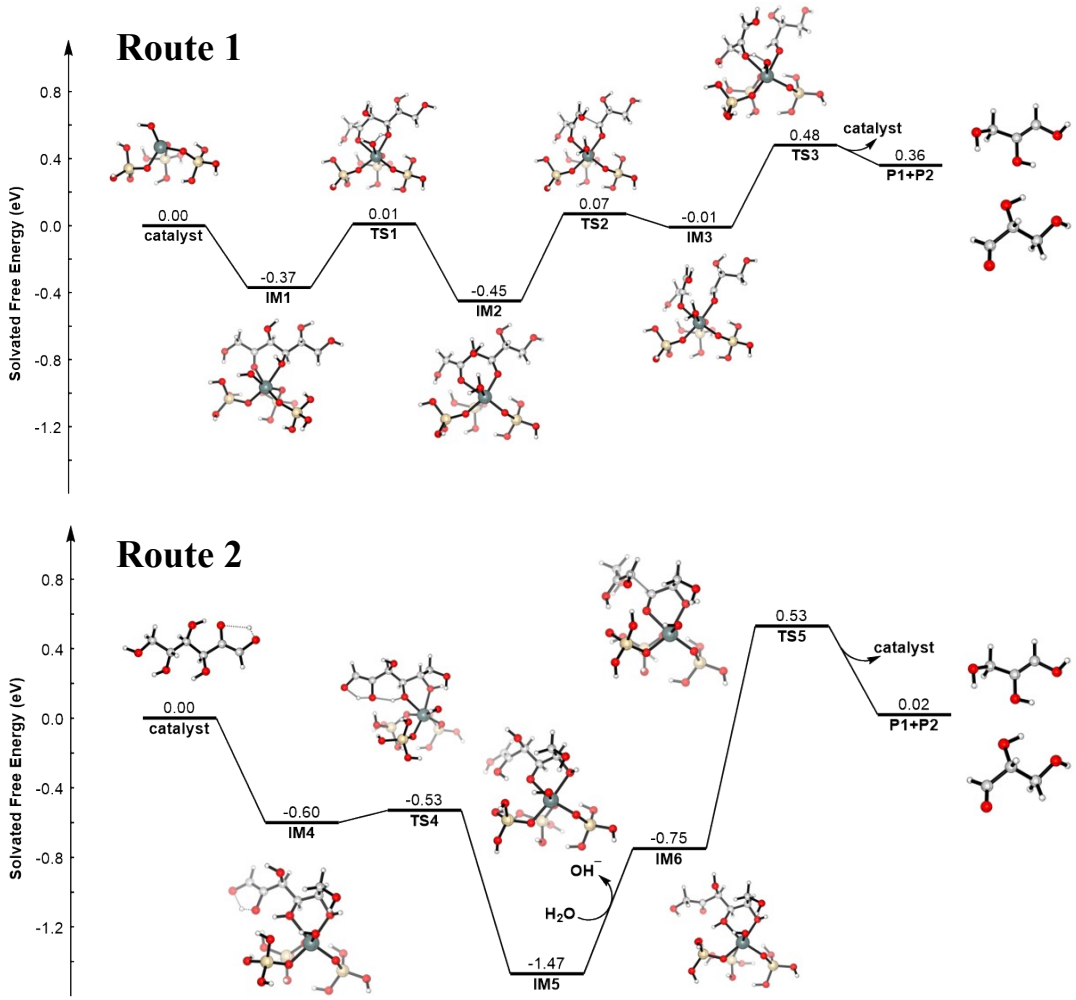

Figure S15. C-C cleavage of two different adsorption models.

Reference

[1] P. J. Stevens, F. J. Devlin, C. F. Chablowski, and M. J. Frisch, *J. Phys. Chem.*, 98 (1994) 11623.
[2] S. Grimme, S. Ehrlich and L. Goerigk, *J. Comp. Chem.* 32 (2011) 1456.
[3] W. J. Hehre, R. Ditchfield and J.A. Pople, *J. Chem. Phys.*, 56 (1972) 2257.
[4] M. M. Francl, W. J. Pietro, W. J. Hehre, J. S. Binkley, M. S. Gordon, D. J. DeFrees and J. A. Pople, *J. Chem. Phys.*, 77 (1982) 3654.
[5] T. Clark, J. Chandrasekhar and P. v. R. Schleyer, *J. Comp. Chem.*, 4 (1983) 294.
[6] M. Dolg, U. Wedig, H. Stoll, and H. Preuss, *J. Chem. Phys.*, 86 (1987) 866.
[7] K. Fukui, *J. Phys. Chem.*, 74 (1970) 4161.
[8] K. Fukui, *Acc. Chem. Res.*, 14 (1981) 363.
[9] F. Weigend, and R. Ahlrichs, *Phys. Chem. Chem. Phys.*, 7 (2005) 3297.
[10] F. Weigend, *Phys. Chem. Chem. Phys.*, 8 (2006) 1057.
[11] J. Tomasi, B. Mennucci, and R. Cammi, *Chem. Rev.*, 105 (2005) 2999.
[12] A. V. Marenich, C. J. Cramer, and D. G. Truhlar, *J. Phys. Chem. B*, 113 (2009) 6378.
[13] Gaussian 16, Revision C.01, Frisch, M. J.; Trucks, G. W.; Schlegel, H. B.; Scuseria, G. E.; Robb, M. A.; Cheeseman, J. R.; Scalmani, G.; Barone, V.; Petersson, G. A.; Nakatsuji, H.; Li, X.; Caricato, M.; Marenich, A. V.; Bloino, J.; Janesko, B. G.; Gomperts, R.; Mennucci, B.; Hratchian, H. P.; Ortiz, J. V.; Izmaylov, A. F.; Sonnenberg, J. L.; Williams-Young, D.; Ding, F.; Lipparini, F.; Egidi, F.; Goings, J.; Peng, B.; Petrone, A.; Henderson, T.; Ranasinghe, D.; Zakrzewski, V. G.; Gao, J.; Rega, N.; Zheng, G.; Liang, W.; Hada, M.; Ehara, M.; Toyota, K.; Fukuda, R.; Hasegawa, J.; Ishida, M.; Nakajima, T.; Honda, Y.; Kitao, O.; Nakai, H.; Vreven, T.; Throssell, K.; Montgomery, J. A., Jr.; Peralta, J. E.; Ogliaro, F.; Bearpark, M. J.; Heyd, J. J.; Brothers, E. N.; Kudin, K. N.; Staroverov, V. N.; Keith, T. A.; Kobayashi, R.; Normand, J.; Raghavachari, K.; Rendell, A. P.; Burant, J. C.; Iyengar, S. S.; Tomasi, J.; Cossi, M.; Millam, J. M.; Klene, M.; Adamo, C.; Cammi, R.; Ochterski, J. W.; Martin, R. L.; Morokuma, K.; Farkas, O.; Foresman, J. B.; Fox, D. J. Gaussian, Inc., Wallingford CT, 2016.